Noritaka Yusa*, Takuma Tomizawa, Haicheng Song, Hidetoshi Hashizume
Tohoku University, Japan

Probability of detection analyses of eddy current data for the detection of corrosion

Prawdopodobieństwo detekcji w wykrywaniu korozji metodą prądów wirowych

ABSTRACT

This study evaluated the applicability of probability of detection (POD) analyses to eddy current tests for the detection of corrosions. Forty-three ferromagnetic plates with various corrosions were prepared, and eddy current inspections were performed to gather signals due to the corrosions using an absolute type pancake probe. The probe scanned the surface of the plates two-dimensionally with a constant lift-off to simulate nondestructive inspection of corrosion under insulating coatings. Subsequent POD analyses adopted two models: a conventional one wherein a flaw was characterized using a single parameter, and a multi-parameter model based on the combinational use of numerical simulations and measurements. The analyses demonstrated that the conventional model would overestimate the probability of detecting small corrosions. In contrast, the multi-parameter model characterized POD more reasonably while its confidence interval was comparable to that of the conventional model.

Keywords: electromagnetic nondestructive evaluation; uncertainty; statistical analysis; ferromagnetic plate; artificial corrosion

STRESZCZENIE

Dokonano oceny przydatności analiz prawdopodobieństwa wykrywania (POD) do wykrywania korozji na podstawie badań metodą prądów wirowych. Przygotowano czterdzieści trzy płytki ferromagnetyczne z różnym stanem skorodowania. Następnie przeprowadzono inspekcje metodą prądów wirowych i zebrano sygnały uzależnione od korozji za pomocą absolutnych sond typu „pancake coil". Sonda skanowała powierzchnie płyt w dwóch wymiarach na stałej wysokości nad materiałem, tak by zasymulować nieniszczącą inspekcję korozji w elementach pokrytych powłokami izolacyjnymi. W kolejnych etapach analizy POD przyjęto dwa modele: konwencjonalny, w którym wada była charakteryzowana za pomocą pojedynczego parametru, a także model wieloparametrowy oparty na kombinacyjnym zastosowaniu symulacji numerycznych i pomiarów. Analizy wykazały, że model konwencjonalny prowadził do przeszacowania prawdopodobieństwa wykrycia małych korozji. Natomiast model wieloparametrowy charakteryzował POD bardziej racjonalnie, a jego przedział ufności był podobny jak w przypadku modelu konwencjonalnego

Słowa kluczowe: elektromagnetyczne badania nieniszczące; niepewność; analiza statystyczna; płyta ferromagnetyczna; sztuczna korozja

1. Introduction

Corrosion of steel is one of the most common degradations observed in various structures[1-4], and thus it is also one of the major targets of nondestructive testing and evaluation in general. Commonly, nondestructive inspections to detect corrosions are scheduled and planned on the basis of certain predictions concerning how the structure will be corroded. However, corrosion prediction is difficult since corrosions are chemical phenomena with various influencing factors[5-8]. Therefore, the validity of the schedule and the plan should be evaluated probabilistically, i.e., from the viewpoint of risk. This indicates the need to evaluate the capability of nondestructive testing methods applied to the detection of corrosion not deterministically but probabilistically, too.

One of approaches that would address this issue is the application of the probability of detection (POD) concept that represents the capability of nondestructive testing methods to detect a flaw probabilistically[9-11]. A problem associated with the application of the conventional POD model is that a flaw needs to be characterized by a single parameter although it is actually difficult to characterize corrosion using just a single parameter[12-14]. A simple extension of the conventional POD model to consider multiple flaw parameters leads to a significant increase in the cost and burden necessary for constructing POD.

Recent studies by the authors have proposed another POD model, the multi-parameter POD model, to consider more than one flaw parameter relatively easily on the basis of a combinational use of numerical simulations and measurements[15,16]. The model does not postulate uniform variance of measured signals or linerality between flaw parameters and signals due to a flaw, which enables modeling of the effect of the flaw parameters on the signals reasonably and naturally. The studies demonstrated the effectiveness of the multi-parameter POD model applied to the POD analysis of artificial slits simulating surface-breaking cracks. However, its applicability to corrosions, the profile of which is much more complicated than artificial slits, has not been evaluated so far.

On the basis of this background, this study evaluated the applicability of the multi-parameter POD model to characterize the detectability of corrosions using eddy current testing. Forty-three magnetic plate samples with artificial corrosion were prepared; signals due to the corrosions were gathered using an absolute type pancake probe driven at 100 kHz with a lift-off of 1.2 mm to simulate eddy current inspection of corrosions under coating. The results of this study confirmed the importance of characterizing corrosion using more than one parameter to obtain a reliable POD.

*Corresponding author. E-mail: noritaka.yusa@qse.tohoku.ac.jp

4

2. Materials and methods

2.1 Samples

Cold-rolled steel plates (JIS G 3141, Grade SPCC) were prepared from various lots to artificially introduce corrosions. The plates measured 100 x 50 mm and had a thickness of 1.94-1.95 mm. After vinyl tape was attached to mask most of the plate surfaces to restrict corrosion area, the plates were soaked into iron(III)-chloride-based etchant H-1000A (Sunhayato Corp., Japan) at 50°C to introduce corrosions. Finally 43 samples with corrosions were prepared; each sample contained a single corroded area approximately at its center.

Table 1 lists the 43 samples prepared. The digits in the ID stand for the duration in hours for which the sample was soaked into the etchant; the characters following the digits are to identify samples having the same duration. The small and large diameter mean the diameter of the largest circle that the corroded area could contain and the diameter of the smallest circle that could encircle the corroded area, respectively, which were measured by a vernier caliper. The maximum depth of the corrosion was measured by a MCD232-25P digital micrometer with tapered tips (Niigata seiki Co., Ltd., Japan).

Neither small nor large diameter showed clear correlation with the depth (correelation coefficient, R = 0.36 and 0.26, respectively). This was because the diameters depended mainly on the area that was not masked by the vinyl tape before the sample was soaked into the etchant. In contrast, the small and the large diameters were strongly correlated (R = 0.83).

Figure 1 shows photographs of six of the corrosions, confirming the variety of corrosion profiles in not only size but also in their significantly different morphologies. The depth of each corrosion is not constant. These indicated that the three parameters of small and large diameter and maximu depth were far from sufficient in providing an accurate representation of corrosion profiles. It should be noted that increasing the number of parameters used to characterize a flaw leads to difficulty in analyzing the effect of the parameters on measured signals; however, it would be reasonable to adopt parameters to characterize the macroscopic profile of a flaw that would affect the integrity of structures.

Fig. 1. Photographs of corrosions introduced into six of the samples. The size of the photographs is 5 cm x 5 cm.
Rys. 1. Fotografie korozji wytworzonych w sześciu próbkach. Rozmiar zdjęć wynosi 5 cm x 5 cm.

Tab. 1. List of samples prepared in this study unit: mm.
Tab. 1. Lista próbek użytych podczas badania.

ID	Small diameter, mm	Large diameter, mm	Maximum depth, mm
3A	5.0	13.3	0.10
3B	16.9	23.4	0.12
3C	24.4	32.7	0.09
3D	11.7	18.1	0.29
5A	17.2	24.2	0.17
5B	9.9	5.6	0.24
5C	5.7	6.4	0.22
7A	17.3	19.2	0.24
7B	23.8	35.3	0.28
7C	6.3	12.0	0.22
10A	25.5	23.6	0.46
10B	8.1	8.2	0.62
16A	19.3	21.9	0.43
16B	30.2	42.8	0.46
16C	35.2	51.7	0.35
16D	22.4	22.6	0.44
16E	45.1	58.1	0.41
16F	27.9	47.8	0.89
18A	23.3	35.2	0.59
18B	25.4	32.5	0.69
24A	14.0	20.6	1.11
24B	19.2	29.8	0.84
24C	9.4	8.1	0.36
24E	30.1	42.6	0.92
24F	25.1	29.0	0.74
24G	21.4	16.3	0.19
24H	23.0	19.1	1.01
27A	32.8	40.4	1.87
31A	33.8	35.3	0.68
35A	2.6	2.7	0.04
35B	3.4	3.3	0.04
35C	40.6	23.9	1.35
35D	34.0	20.0	0.86
40A	26.9	28.7	0.49
41A	36.8	48.6	0.85
41B	32.5	53.3	1.59
41C	25.9	27.1	1.14
64A	30.0	33.4	1.10
71A	16.5	16.2	1.95
71B	19.4	26.4	1.91
71C	20.0	39.0	0.97
71D	25.6	21.8	1.80
71E	13.3	17.3	1.57

2.2 Eddy current examination

Eddy current examinations were conducted using the aect2000N commercial eddy current instrument (Aswan ECT Co. Ltd., Osaka, Japan), and an absolute type pancake probe with a height, inner diameter and outer diameter of 0.8, 1.2, and 3.2 mm, respectively. The excitation frequency was 100 kHz. The probe was attached to an XYZ-stage controlled by a PC, for two-dimensional scanned of the surface where the corrosion was introduced, with a lift-off of 1.2 mm to simulate eddy current inspection of corrosions under insulating

coatings. The pitch of the scanning is 2 and 3 mm in the lateral and longitudinal directions of the sample, respectively.

2.3 POD analysis

This study adopted two POD models: a conventional POD model and a multi-parameter POD model.

The conventional POD model assumes linearity between the 'size' of a flaw, a, and the amplitude of signals, $\hat{a}$, whereas proper transformation, typically log-transform, is applied when it is difficult to confirm the linearity between them. After $\hat{a}$ is represented as a probabilistic function of a, the probability that the probabilistic function exceeds a given threshold, a_{th}, provides the probability that a flaw with a size of a is detected, $P(a) = P(\hat{a} > a_{th})$. More detailed and specific procedures can be found in the ASM and USDOD Handbooks[10,11]. It should again be emphasized that this model characterizes a flaw using a single parameter.

The multi-parameter POD model assumes that measured signals due to a flaw with profile represented by a vector $\vec{a}$ are represented as:

$$V(\vec{a}) = N(\mu_1, \sigma_1^2)V^{sim}(\vec{a}) + N(\mu_2, \sigma_2^2)$$

where $V(\vec{a})$ and $V^{sim}(\vec{a})$ are the maximum amplitude of signals obtained from experiments and by numerical simulation, respectively.

In this study, axisymmetric finite element simulations were performed to obtain $V^{sim}(\vec{a})$. In the simulations, a corrosion was simply modeled as a cylindrical void situated directly below a probe; the parameters used in the simulations are summarized in Tab. 2. It should be noted that the elements of $\vec{a}$ are flaw parameters that can be explicitly modeled in numerical simulations, and that the simulation does not assume the distribution of noise sources to evaluate noise[17-20]. The effect of uncertainty and noise are represented by two normal distributions, $N(\mu, \sigma^2)$, where μ and σ stand for the mean and standard deviation. The four parameters, μ_1, σ_1, μ_2, and σ_2, characterizing the uncertainty and noise are evaluated by likelihood analysis on the basis of $V(\vec{a})$ and $V^{sim}(\vec{a})$; the probability of detection is given as the probability that $V(\vec{a})$ exceeds a given threshold a_{th}, $P(\vec{a}) = P(V(\vec{a}) > a_{th})$. More detailed procedures to evaluate the four parameters are described in the earlier publications[15,16]

Tab. 2. Parameters used for the simulations to obtain $V^{sim}(\vec{a})$.
Tab. 2. Parametry użyte w symulacji w celu otrzymania $V^{sim}(\vec{a})$.

Parameter	Value
Conductivity of plate, MS/m	6.0
Relative permeability of plate	100
Diameter of the void, mm	1, 3, 5, 10, 20, 30, 40, 46
Depth of the void, mm	0.03, 0.06, 0.10, 0.20, 0.30, 0.40, 0.50, 0.60, 0.70, 0.80, 0.90, 1.00, 1.10, 1.20, 1.30, 1.40, 1.50, 1.60, 1.70, 1.80, 1.90, 1.93, 1.96

3. Results and discussion

Figure 2(a) summarizes the amplitude of the signals measured in the experiments, $V(\vec{a})$. The amplitudes were normalized so that the amplitude of the signal due to the sample with the deepest corrosion, 71A, was 1.0. This figure, together with Tab. 1, revealed that 'large' corrosions do not always provide larger signals. Although a finer scanning pitch would have changed the measured signals, the most plausible reason for this observation is that the three parameters do not fully represent the corrosion profile, as discussed above. Figure 2(b) presents the amplitude of simulated signals, $V^{sim}(\vec{a})$, which are obtained by interpolating the results of the numerical simulations. Whereas the two figures would be qualitatively similar to each other, the figures reveal the difficulty in quantitatively evaluating signals due to corrosions. This implies that it would not be reasonable to use numerical simulations just to increase the amount of data for POD analysis.
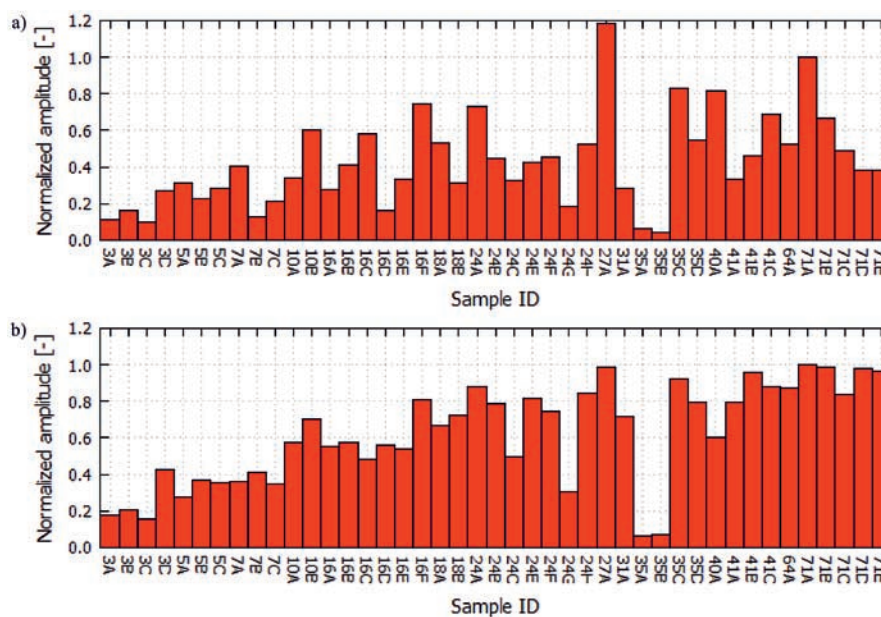

Fig. 2. Amplitude of the signals: a) measurement; b) simulation.
Rys. 2. Amplitudy sygnałów:) pomiar; b) symulacja.

The results of the conventional POD analyses are summarized in Figs. 3-5. All of the parameters and the signal amplitude were log-transformed on the basis of several preliminary tests to evaluate the linearity between a flaw parameter and the signal amplitude. Figures 3 and 4 reveal that PODs as a function of the small or large diameter were not reliable because of their large confidence intervals. The results of the regression analyses showed relatively large standard deviations, indicating that the parameters were not the most dominant ones affecting the signals. In contrast, POD as a function of the maximum depth, which is shown in Fig. 5, showed a much narrower confidence interval that

implied the validity of the POD. It should be noted, however that Figs. 3 and 4 indicate that the diameters should influence the signals as well as POD because the diameters have little correlation with the depth.
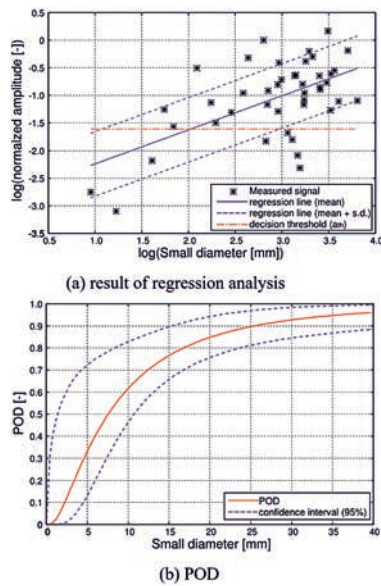

Fig. 5. Results of regression and POD analyses when the depth was used as a parameter to characterize corrosion.
Rys. 5. Wyniki regresji i analizy POD dla przypadku, gdy jako parametru charakteryzującego korozję użyto głębokość.

Confirming this is Fig. 6, which shows the effect of the parameters on signals using the results of the numerical simulations to obtain $V^{sim}(\vec{a})$. Because the simulations were conducted using the axisymmetric model, a corrosion was modeled as a cylindrical void with a diameter of φ and constant depth, as stated above. As can be seen, when the diameter was smaller than 5 mm, its effect was not negligible. Thus, considering only the depth of a corrosion is not sufficient especially in evaluating the probability of detecting small flaws.

Fig. 3. Results of regression and POD analyses when the small diameter was used as a parameter to characterize corrosion.
Rys. 3. Wyniki regresji i analizy POD dla przypadku, gdy jako parametru charakteryzującego korozję użyto małą średnicę.
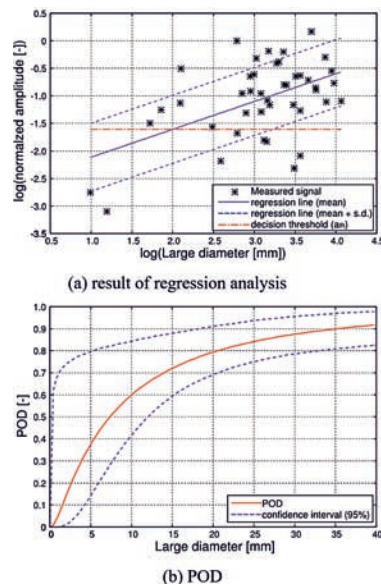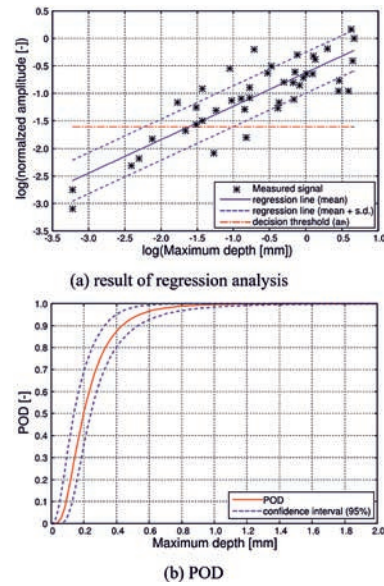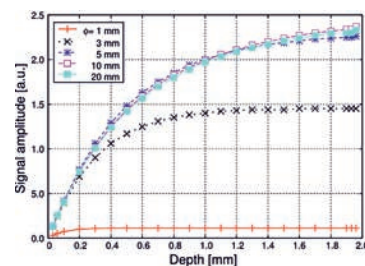

Fig. 6. The effect of the diameter of the void, φ, on the relationship between the depth of the void and the amplitude of the signal due to the void.
Rys. 6. Wpływ średnicy pustki, φ, na zależność między głębokością pustki a amplitudą sygnału wywołanego pustką.

Figure 7 shows the POD as a function of both the small diameter and the depth of corrosion; its confidence interval is presented in Fig. 8. The four contour lines on the base planes of the figures correspond to POD = 0.3, 0.5, 0.7 and 0.9. The strong correlation between the small and large diameters implied that using the large diameter instead of the small one would lead to a similar result, whereas the confidence intervals shown in Figs. 3 and 4 supported the validity of using the small diameter.

Fig. 4. Results of regression and POD analyses when the large diameter was used as a parameter to characterize corrosion.
Rys. 4. Wyniki regresji i analizy POD dla przypadku, gdy jako parametru charakteryzującego korozję użyto dużą średnicę.

The POD presented in Fig. 7 highlights the difficulty in detecting a deep corrosion if its small diameter is as small as a few millimeters, which is consistent with the findings from Fig. 6. The confidence interval of the POD corresponded to change in a maximum depth of approximately 0.2 mm if the small diameter of corrosion was larger than a few millimeters. This was comparable with that of the conventional POD shown in Fig. 5(b).
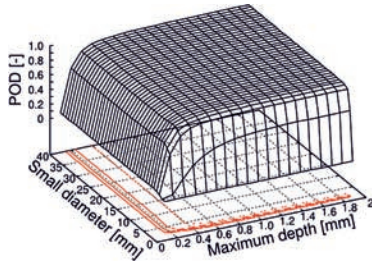

Fig. 7. Two-dimensional POD obtained as a function of both small diameter and maximum depth of corrosions.
Rys. 7. Dwuwymiarowy rozkład POD uzyskany w funkcji zarówno małej średnicy, jak i maksymalnej głębokości korozji.

(a) lower confidence bound

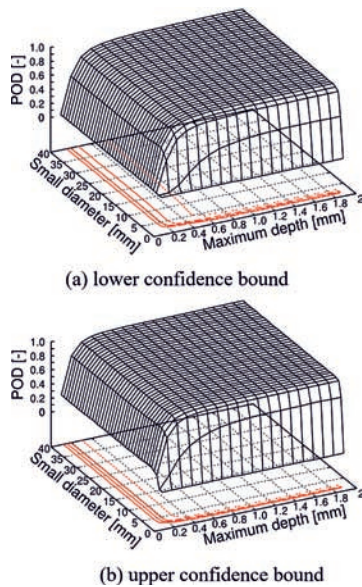(b) upper confidence bound

Fig. 8. Fig. 8 Confidence interval of the two-dimensional POD shown in Fig. 7.
Rys. 8. Przedział ufności dwuwymiarowego rozkładu POD pokazanego na rys. 7.

4. Conclusion

This study evaluated the applicability of POD analyses to eddy current inspection for corrosion detection. Ferromagnetic plates with artificial corrosions were prepared; eddy current testing using an absolute type pancake probe was conducted to simulate inspection of corrosions under insulating coatings. Two POD models were applied: a conventional one that characterized a flaw using a single parameter, and a multiparameter model based on a combinational use of numerical simulations and measurements. The results of this study confirmed that conventional model would overestimate the POD of small corrosions while the multi-parameter model characterized the POD more reasonably.

5. References/Literatura

[1] RE. Melchers, "Recent progress in the modeling of corrosion of structural steel immersed in seawaters", Journal of Infrastructure Systems, vol. 12, no. 3, pp. 154-162, 2006.

[2] HR. Vanaei, A. Eslami, A. Egbewande, "A review on pipeline corrosion, in-line inspection (ILI), and corrosion growth rate models", International Journal of Pressure Vessels and Piping, vol. 149, pp. 43-54, 2017.

[3] W. Ferdous, A. Manalo, "Failures of mainline railway sleepers and suggested remedies –Review of current practice", Engineering Failure Analysis, vol. 44, pp. 17-35, 2014.

[4] SJ. Findlay, ND. Harrison, "Why aircraft fail", Materials Today, vol. 11, 18-25, 2002.

[5] F. Caleyo, JL. Gonzalez, JM. Hallen, "A study on the reliability assessment methodology for pipelines with active corrosion defects", International Journal of Pressure Vessels and Piping, vol. 79, pp. 77-86, 2002.

[6] Y. Sahraoui et al. "Maintenance planning under imperfect inspections of corroded pipelines", International Journal of Pressure Vessels and Piping, vol. 104, pp. 76-82, 2013.

[7] S. Zhang, W. Zhou, "System reliability of corroding pipelines considering stochastic process-based models for defect growth and internal pressure", International Journal of Pressure Vessels and Piping, vol. 111-112, pp. 120-130, 2013.

[8] MR. Dann, L. Huyse, "The effect of inspection sizing uncertainty on the maximum corrosion growth in pipelines", Structural Safety, vol. 70, pp. 71-81, 2018.

[9] C. Annis, J.C. Aldrin, A. Sabbagh, "NDT Capability - What is missing in nondestructive testing capability evaluation?", Materials Evaluation, vol. 73, no. 3, pp. 44-54, 2015.

[10] AP. Berens, NDE Reliability data analysis, ASM Handbook, Volume 17: Nondestructive Evaluation and Quality Control: ASM International, pp. 689-670, 1989.

[11] Department of Defense Handbook: Nondestructive Evaluation System Reliability Assessment: USDOD, MIL-HDBK-1823A, 2009.

[12] J. Kim, M. Le, J. Lee, YH. Hwang, "Eddy current testing and evaluation of far-side corrosion around rivet in jet-engine intake of aging supersonic aircraft", Journal of Nondestructive Evaluation, vol. 33, pp. 471-480, 2014.

[13] R. Howard, F. Cegla, "On the probability of detecting wall thinning defects with dispersive circumferential guided waves", NDT&E International, vol. 86, pp. 73-82, 2017.

[14] J. Kim, et al. "Nondestructive evaluation of far-side corrosion around a rivet in a multilayer structure", Research in Nondestructive Evaluation, vol. 29, no. 1, pp. 18-37, 2018.

[15] N. Yusa, J. Knopp, "Evaluation of Probability of Detection (POD) studies with multiple explanatory variables", Journal of Nuclear Science and Technology, vol. 53, no. 4, 574-579, 2016.

[16] N. Yusa, W. Chen, H. Hashizume, "Demonstration of probability of detection taking consideration of both the length and the depth of a flaw explicitly", NDT&E International, vol. 81, pp. 1-8, 2016.

[17] J.C. Aldrin, et al. "Demonstration of model-assisted probability of detection evaluation methodology for eddy current nondestructive evaluation", AIP Conference Proceedings, vol. 1430, pp. 1733-1740, 2012.

[18] RM. Meyer, JP. Lareau, SL. Crawford, MT. Anderson, "Review of literature for model assisted probability of detection", PNNL-23714:2014.

[19] JS. Knopp, R. Grandhi, JC. Aldrin, I. Park, "Statistical analysis of eddy current data from fastener site inspections", Journal of Nondestructive Evaluation, vol. 32, pp. 44-50, 2013.

[20] PN. Bilgunde, LJ. Bond, "Model-assisted approach for probability of detection (POD) in high-temperature ultrasonic NDE using low-temperature signals", Nuclear Technology, vol. 202, pp. 161-172, 2018.